A&A 411, 167–180 (2003)
DOI: 10.1051/0004-6361:20031179

Astronomy & Astrophysics

Stellar and circumstellar activity of the Be star ω CMa*

II. Periodic line-profile variability

S. Štefl[1], D. Baade[2], Th. Rivinius[2,3], O. Stahl[3], A. Budovičová[1], A. Kaufer[2], and M. Maintz[3]

[1] Astronomical Institute, Academy of Sciences, 251 65 Ondřejov, Czech Republic
[2] European Southern Observatory, Karl-Schwarzschild-Str. 2, 85748 Garching bei München, Germany
[3] Landessternwarte Königstuhl, 69117 Heidelberg, Germany

Received 8 April 2003 / Accepted 25 July 2003

Abstract. The rapid line-profile variability of the early-type and pole-on Be star ω CMa between 1996 and 2002 is characterized across the complete optical spectrum, for quiescent phases as well as for outbursts. Owing to different and changing line-profile variability patterns, amplitudes and γ-velocities are different from line to line and are variable on a time scale of months. A comprehensive time series analysis was performed on the modes of a set of selected lines (after individual seasonal normalization to avoid biases). At a high level of confidence, only the well-known 1.37-d period could be found in photospheric lines not contaminated by the disk. Outside major outbursts, when the star is at its photometric ground state, the phase coherence of the variability is very robust. During strong outbursts, when the star is visually bright, the period may either be very slightly different or phase jumps may occur. The present observations do not have the sampling necessary to distinguish between these possibilities. Harmanec's (1998) report of continuous, cyclic period variations cannot be confirmed. Arguments are presented that temporary period changes may be related to interactions between the photospheric non-radial pulsation and the disk when (during outbursts) these two domains are in contact with one another. This result does not seem to be an artifact of the also previously reported transient periodicities near 1.49-d, which are prominent during outbursts and seem to be anchored in the exo-photosphere. However, if not properly taken into account, they may easily lead to false conclusions about multiple or variable periods. In the Be star μ Cen, which has a similar spectral type, outbursts are triggered by the beating of two or more non-radial pulsation modes (Rivinius et al. 1998b). Since ω CMa, too, undergoes outbursts although its photospheric variability is single-periodic, the case of μ Cen cannot be generalized to the activity of all early-type Be stars or to the Be phenomenon at large.

Key words. stars: activity – stars: circumstellar matter – stars: emission-line, Be – stars: individual: ω 28 CMa

1. Introduction

In the first paper of this series (Štefl et al. 2003, hereafter Paper I) the photometric and spectroscopic long-term behavior of ω CMa was analyzed. Special consideration was given to phases of high brightness, which develop semi-regularly every 7–9 years. The results indicate that the matter is supplied to the circumstellar disk mainly in the form of discrete events (outbursts). The resulting changes in the density and density distribution of the disk on time scales of months to years reveal themselves by photometric and spectroscopic variations, which are also known from other early-type Be stars. The brightness maximum is observed when the density is highest in the inner parts of the disk and continuum flux is strongly scattered also towards the line of sight. The Hα emission becomes maximal only later when the ejected matter reaches the outer disk (and has sufficiently cleared the inner disk for the stellar flux to ionize the outer disk). The area of the Hα emitting disk is then largest. Because the disk is largely optically thick in Hα, this maximizes the strength of the Hα line emission. During such bright states other phenomena may occur as well, e.g. cyclic light variations on a time scale of 20 days and highly redshifted components in some spectral lines. They are not seen when the star is in its photometric ground state.

This second paper of the series is devoted to line-profile variability (*lpv*) on much shorter time scales of hours to days. Variations with periods of 0.5–2.0 days are ubiquitous among early-type Be stars. It was, therefore, conjectured that they are directly linked to the development of disks around very rapidly rotating B stars. This suspicion was strengthened after Rivinius et al. (1998b) found a correlation between the times of line emission outbursts and the times of beating of the strongest non-radial pulsation (*nrp*) modes in the Be star μ Cen. But to

Send offprint requests to: S. Štefl,
e-mail: sstefl@pleione.asu.cas.cz

* Based on observations collected at the European Southern Observatory at La Silla, Chile (ESO proposals No. 55.D–0502, 56.D–0381, 58.D–0697, 64.H–0548, 62.H–0319 and 267.D–5702).

date, the only other stars, which have been identified as candidates for a similar behavior, are 28 Cyg (Tubbesing et al. 2000) and η Cen (Rivinius et al., in preparation). This warrants an in-depth time-series analysis of more Be stars. The bright prototypical line profile-variable Be star ω CMa suggests itself for such a study.

The *lpv* of ω CMa was repeatedly confirmed to be periodic with $P = 1.3667 \pm 0.007$ d ($f = 0.733 \pm 0.004$ cycle d^{-1}; Baade 1984). In particular, Harmanec (1998) compiled all published radial velocities and derived a more accurate period from the times of RV minima. After careful discussion, he concluded that the exact value of the period varies cyclically on a time scale of 5650 ± 400 days about the mean value of 1.372 d with a semi-amplitude of $0.174 \pm .017$ day. No other check of the long-term stability of the 1.37-d period was performed to date. In particular, no attempt has been made to investigate whether the variability associated with the 1.37-d period is somehow dependent on the long-term variability. Even in the case that the 1.37-d variability is unrelated to the origin of the Be phenomenon, its time depencency could provide important diagnostics of the nature of the long-term variability.

A detailed investigation of high-resolution He I 6678 line profiles was presented by Štefl et al. (1999). Their data, spread only over an interval of 10 days, did not allow to look for periods other than the 1.37-d period. But they could find strong indications, both in line profile and light variations, of the presence of a 1.49-d period previously reported by Štefl et al. (1998) from observations in 1996 for an independent project.

As for other Be stars, the first analyses of the rapid *lpv* of ω CMa were mainly limited to one He I line only. In addition, it was implicitly assumed that the corresponding *lpv* pattern was dependent on neither spectral line nor epoch. Later, work on μ Cen and preliminary inspection (Štefl et al. 1998, 2000b) of subsets of the data used in this study revealed a more complex picture:

- In spectral lines formed in the photosphere and having no circumstellar contribution, some period(s) can always be detected.
- Secondary, so-called transient periods may appear in spectral lines that do have a significant circumstellar contribution. Their power is negligible or small in He I lines, but can be entirely dominant in lower lines of the H I Balmer series. Line wings are more strongly affected than are line cores. In μ Cen it appears that transient periods occur during or shortly after outbursts and fall in a relatively narrow interval of about $\pm 10\%$ of the dominating photospheric period. During different outbursts they can assume significantly different values. (Rivinius et al. 1998b). At any given epoch, only one transient period was detected.
- Transient periods can severely compromise the significance of the results of long-term time series analyses if not properly taken into account.

A period search in ω CMa is further complicated by differences in the RV amplitude between different ions and, for a given ion, between seasons (Baade 1984; Štefl et al. 2000b).

Maintz et al. (2000) showed that even fine details of the rapid *lpv* of ω CMa can be modeled as low-order *nrp* (with $\ell = 2$, $m = +2$). In particular, like in the observations, the calculated *lpv* patterns vary considerably from line to line. This results from equator-to-pole gradients of effective temperature and electron pressure in a rapidly rotating star (for more details see Maintz et al. 2003).

In the present paper, a time series analysis (TSA) of the rapid *lpv* is undertaken using the full data set described in Paper I. An overview of the behavior of specific spectral lines is given in Sect. 2. Section 3 presents the TSA of radial velocities of photospheric absorption lines; it is complemented in Sect. 4 by the TSA of likewise scalar parameters of emission lines. Sharp absorption spikes, which develop at specific phases of the *lpv* are described in Sect. 5. The results are discussed in Sect. 6. Finally, Sect. 7 attempts to accommodate the considerable diversity of line- and epoch-specific phenomena in one generalized scheme.

2. Phenomenology of the rapid line profile variability

2.1. Loci of formation of various spectral lines

The list of spectral lines used for the analysis in this paper is given in Table 1. The last column contains a crude indication of the "place of formation" of the line. In a star with a very extended atmosphere, this is by necessity an oversimplification. *All* studied lines have a significant to strong photospheric component. To varying degrees they are affected by the radiation transfer processes in the transition region above the photosphere and in the disk itself. Excitation of the gas in the disk can lead to the formation also of emission components. The exact determination of the photospheric and exo-photospheric contributions to each line profile would require solving the radiation transfer equations in an extended, variable stellar atmosphere. For the given purpose of identifying possible differences, if any, in the basic place of origin of various processes this is not needed.

The approximative classification scheme is based on the following qualitative arguments:

- Variability matching the one of indisputable emission lines is a key indicator of at least some circumstellar contribution.
- Spectral lines with high excitation potential stand a low chance of being significantly affected by the disk.
- Regions of line and continuum emission can be directly mapped by interferometric observations. Stee (2000) used the GI2T/REGAIN interferometer to measure the disk radius of γ Cas at different wavelengths. While the Hα emission disk extends up to 18 $R_\star$, it is only 8.5 and 2.3 $R_\star$ in Hβ and in He I 6678, respectively. Such results provide some crude scaling relations.
- The emission components of H I Balmer and Paschen lines and O I 8446 are formed in the disk following Bowen pumping of their upper atomic levels.
- To first approximation, He I emission lines are well accounted for by models of a dense stellar wind (Najarro 1995).

Table 1. The spectral lines used for the time series analysis. "low" and "up" denote excitation energies of the lower and upper atomic level, respectvely. The last column contains a crude indication of the place of formation of the line. Note that *all* lines have a photospheric component: a "p" identifies this to be the dominant one by far. "c" signals some circumstellar contribution, and lines marked "sc" – are strongly influenced by processes in the circumstellar disk.

Ion	λ [Å]	low [eV]	up [eV]	log gf	phot/circ contr.
H I	3734.370	10.15	13.45	−1.8737	c
H I	3750.154	10.15	13.45	−1.7643	c
H I	3770.632	10.15	13.43	−1.6443	c
H I	4101.737	10.15	13.16	−0.7527	sc
H I	4340.468	10.15	13.00	−0.4469	sc
H I	4861.332	10.15	12.69	−0.0202	sc
H I	6562.817	10.15	12.04	+0.7098	sc
H I	8545.384	12.04	13.48	−1.4952	sc
He I	3819.606	20.87	24.11	−0.7140	p
He I	3926.530	21.13	24.27	−1.6480	p
He I	4009.270	21.13	24.21	−1.4730	p
He I	4026.200	20.87	23.94	−0.3700	p
He I	4120.800	20.87	23.87	−1.4830	p
He I	4143.759	21.13	24.11	−1.1950	p
He I	4168.971	21.13	24.09	−2.3380	p
He I	4387.928	21.13	22.94	−0.8830	p
He I	4437.550	21.13	23.91	−2.0340	p
He I	4471.477	20.87	23.63	+0.0520	p
He I	4713.200	20.87	23.49	−0.9730	p
He I	4921.929	21.13	23.63	−0.4350	p
He I	5015.680	20.53	22.99	−0.8199	p
He I	5047.739	21.13	23.57	−1.6020	p
He I	5875.700	20.87	22.97	+0.7390	p,c
He I	6678.150	21.13	22.97	+0.3290	p,c
He I	7065.190	20.87	22.62	−0.2050	p,c
Ne I	6402.246	16.55	18.48	+0.2700	p
O I	8446.350	9.48	10.94	+0.4300	sc
Mg II	4481.137	8.83	11.58	+0.9780	c
Si II	6347.109	8.09	10.03	+0.2250	c
Si II	6371.372	8.09	10.02	−0.0740	c
Si III	4552.616	20.87	22.62	+0.2900	p
Fe II	4233.172	2.58	5.51	−1.840	sc
Fe II	4508.283	2.84	5.58	−2.310	sc
Fe II	4549.474	2.82	5.83	−1.96	sc
Fe II	5169.033	2.88	5.27	−1.30	sc
Fe II	5316.615	3.14	5.46	−1.96	sc

In agreement with these considerations, Ne I 6402 and Si III 4553 are lacking emission components not only in ω CMa but in the complete HEROS database. They are the purest examples of photospheric lines not influenced by the circumstellar disk. At the other extreme, Hα and O I 8446 photons are emitted as parts of a cascade following the resonant absorption of stellar continuum flux by Lβ. The expected correlation between the strengths of Hα and O I 8446 was observationally confirmed by Briot (1981).

The profiles of most He I lines are negligibly influenced by the disk. Only in some of them, appreciable line emission occurs. This depends strongly on the disk density and appears to be confined mainly to times of high brightness. At electron densities of $10^{10.5}$–10^{12}, the radiation causes a net pumping of electrons from the 1^{1S}, 2^{1S} singlet and 2^{3S} triplet levels, populating all upper 1-states above their LTE values. The lines marked as "p,c" in Table 1 are the lowermost of the respective fluorescence cascades in the visible spectral range (together with He I 7281, which is veiled by telluric lines in ground based spectra). They should show the strongest emission components, in agreement with observations.

2.2. Spectral line-specific patterns

Figure 1 compiles power and phase distribution across some selected spectral lines. Only observations from the high brightness phase in 1996 are used because, then, the line-to-line differences were most conspicuous. The four lines shown are representative of four groups of lines that are described in the following.

First, regardless of the brightness or the line emission level, Si III 4553 and Ne I 6402 always vary with the 1.37-d period only. Second, moving on to He I lines, one can in their wings see (Fig. 1) incipient power from the transient 1.49-d period (see Sect. 4). This is most pronounced in He I 6678, the lower atomic level of which is always well populated by the extremely strong He I 584 Å transition and which is probably formed also in the inner parts of the circumstellar disk. All He I lines have in common that there is no appreciable 1.49-d power at their line centers and the double-peak power distribution and prograde phase progression are unaltered w.r.t. the pure photospheric case.

Next, rather significant circumstellar contributions can be recognized in Mg II, Si II and higher lines of the Balmer series. The Fourier power of the 1.49-d period remains concentrated in the line wings, but it is noticably stronger than in the He I lines. Also, it is rather asymmetrically distributed, signalling that there is much more variability in the blue than the red line wing. The power of the 1.37-d variability shows a double peak distribution similar to the ones of the photospheric and He I lines.

Finally, lower lines of the Balmer and Paschen series as well as O I and Fe II lines are observed with a net emission and so are formed predominantly in the disk. Their TSA shows the 1.37-d and 1.49-d periods to be of comparable power. The latter may even dominate and usually extends well beyond the "rotationally permitted" range $\pm v \sin i$. During phases of high brightness, some of these lines show a multi-peak power distribution (e.g., Hα) or a particularly strong concentration of the variability in the blue wing. Unlike the previous three groups of lines, the transient periodicity is present not only in the line wings but is well detectable also near the line centers.

All lines represented in the first three panels of Fig. 1 show the same prograde phase propagation across the line profile.

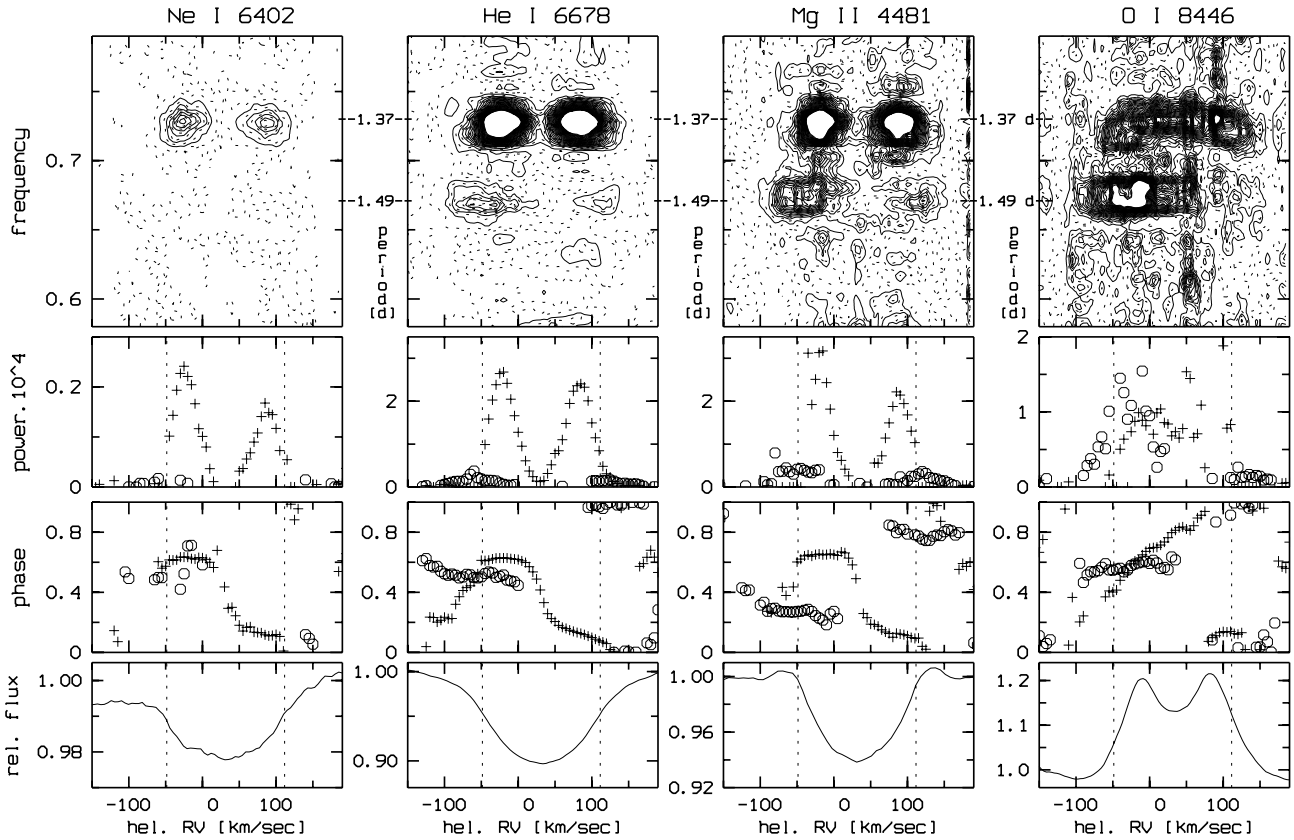

Fig. 1. Frequency analysis of the *lpv* in selected spectral lines during the 1996 observing run. Two-dimensional Fourier diagrams are shown in the uppermost panels, with isophotes connecting points of the same Fourier power. In the next two panels, depicting the power and phase distribution across the line profile, the crosses correspond to the 1.37-d period, circles to the transient 1.49-d period. The lowermost panels display the mean profiles. Dotted vertical lines indicate $\pm v \sin i = 80\,\mathrm{km\,s^{-1}}$, corrected for the systemic velocity of the star of $31\,\mathrm{km\,s^{-1}}$ derived by Štefl et al. (1999). The power of the transient period increases with contribution from the circumstellar disk to the observed profiles.

However, a completely different, retrograde phase propagation can be noticed in lines with the highest contribution from the circumstellar disk (see Fig. 1, Panel 4 and Fig. 3, Panel 1 and the next subsection). Note that in the present data sets retrograde moving features were not seen outside the 1996 observing season when the star was bright.

The above simplified classification scheme of the periodic *lpv* involves the emission line strength and so requires that long-term variations are taken into account (see Paper I). E.g., the strength of Fe II emission lines can drop to below the level of detectability during phases of low activity. The significance of the transient 1.49-d period fades with the strength of the emission components.

2.3. Temporal variations of lpv patterns

Figure 2 shows the 1.37-d *lpv* characteristics of the photospheric Si III 4553 in different seasons. Most *lpv* parameters remain constant through the cycle of long-term variability. During the high brightness in 1996 and the small emission outbursts in 2000, the power distribution was more asymmetric, with more power in the blue wing. The inhomogeneous phase distribution of the spectra taken in 2001/2, when ω CMa was again bright, makes it impossible to check if variability dominating the blue wing of photospheric lines is typical of photometrically bright states.

Much larger season-to-season variations can be seen in Fourier diagrams of lines with major circumstellar contribution such as Mg II and Si II. The main difference is in the strength of the transient periodicity, which is highest and well defined in phases of high brightness and almost disappears during the photometric ground state. The observations in 2000 cover only part of a small outburst and do not show unambiguously the presence of the transient period. The low number of spectra and their temporal distribution do not allow a search for transient periodicities in the 2001/2 dataset. However, additional variability over and above the normal 1.37-d period is certainly present.

In Balmer lines and emission lines of O I 8446 and Fe II, the disappearance of the 1.49-d periodicity during the descent to the photometric ground state is accompanied by a gradual change of the phase progression of the 1.37-d period. Figure 3 illustrates this trend for Hδ. During the 1996 strong activity, the H I lines could be distinguished from most of the other spectral lines by a retrograde progression. Such a phase distribution seems to be typical of these lines during times of high brightness. Only after the photospheric activity has decreased, does the phase distribution return to a prograde one. A transition between these two states was recorded with the 1997

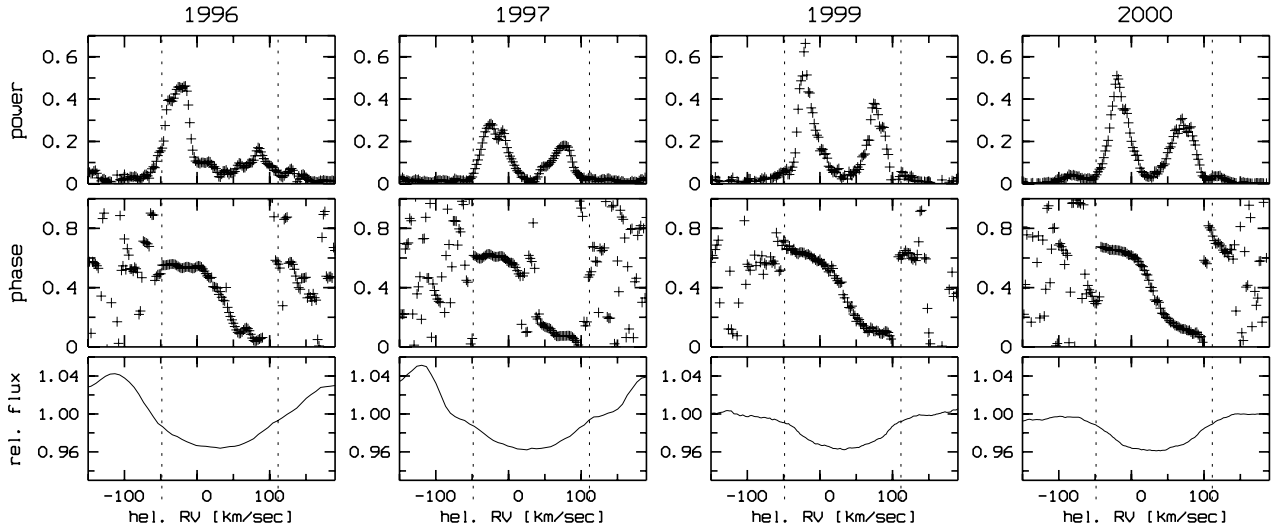

Fig. 2. Time series analysis of the photospheric Si III 4553 line observed in different seasons. Line emission in 1996 and 1997 seasons is due to Fe II lines located almost symmetrically to the Si III line center. The Si III absorption line profile remains nearly constant.

observations (see Fig. 3, Panel 2). In 1999, all Balmer lines shortward of Hβ already showed the normal prograde progression, similar to spectral lines that have a limited circumstellar contribution at all times.

Considerable season-to-season variations can be noticed in the asymmetry of the 1.37-d power distribution. The deviations from the double peak structure are larger during the 1996 outburst and spectral line-dependent. For instance, Hα exposed a single peak distribution in 1996, with its maximum at the line center. It transformed itself to a complicated multiple-peak distribution in the next seasons.

3. Radial velocity of absorption lines

3.1. Measurements and normalization of modes

The definition of the radial velocity (RV) of a pulsating atmosphere is ambiguous in the literature (see, e.g., the discussion in Štefl et al. 1999). In this study, the mode was used, i.e. the position of the maximum/minimum flux within a given emission/absorption line. The values were determined by fitting a Gaussian in a region defined interactively with a graphical cursor. Only the very line core (about 5–10% of the whole profile) was fitted, trying to avoid possible spikes or other aperiodic narrow features. In this way, every derived value could be checked carefully. A total of 25 absorption lines were measured in all available HEROS and FEROS spectra.

A combined TSA of modes measured in different lines and for different years is severely hampered by the variability of the RV amplitudes from season to season and from ion to ion even in a given season (Baade 1984; Štefl et al. 2000b). Figure 4 illustrates this so far only marginally understood fact by the examples of the He I 4009 and 6678 Å lines. Therefore, in a first approximation, the measured modes were sorted with the period of 1.37187 d derived from the scaled mode values of the HEROS 1996 and 1997 data (Štefl et al. 2000b). For each spectral line and in every season, the phase diagram was fitted with a sinusoid, $A + B\sin(C + 2\pi\phi)$, where the phase ϕ is the independent variable and A, B, C are constants to be derived in the fit. The Newton-Raphson method implemented in the standard MIDAS FIT package (Schwarzenberg-Czerny 1993) was applied. The constant C includes possible uncertainties of the period over long time scales and, to first order, possible phase shifts between individual lines and seasons. The constants A and B, respectively, correspond to the systemic velocity, γ, and the amplitude of the radial velocity curve. Table 2 lists the results for each spectral line and observing season.

The line profiles published by Štefl et al. (2000a,where an automatic method was used) and by Baade (1984) were remeasured in the same way as all other spectra, thereby maximizing the homogeneity of the database. Results of the sinusoid fits are provided in Table 3.

The following conclusions can be drawn from Tables 2 and 3:

- RV amplitudes as well as γ-velocities are significantly different for different spectral lines, even for lines of the same ion and observed in the same season.
- The seasonal variations of RV amplitudes are at most little correlated with the general line emission level, i.e. with phase of the long-term variability.

The fitting of phase diagrams did not reveal any significant phase shifts between individual spectral lines. Accordingly, for the next step of the TSA, the mode variations of every ion and season were normalized and shifted to $\gamma = 0$ by adjusting constants A and B in order to enable a comprehensive long-term analysis.

3.2. Time series analysis of combined mode variations

The normalized modes of the HEROS and FEROS spectra from the various seasons were combined and subjected to a period analysis. By keeping individual spectral lines separate, any assumption about the presence or not of phase shifts between different ions was avoided. Scargle's (1982) method was adopted

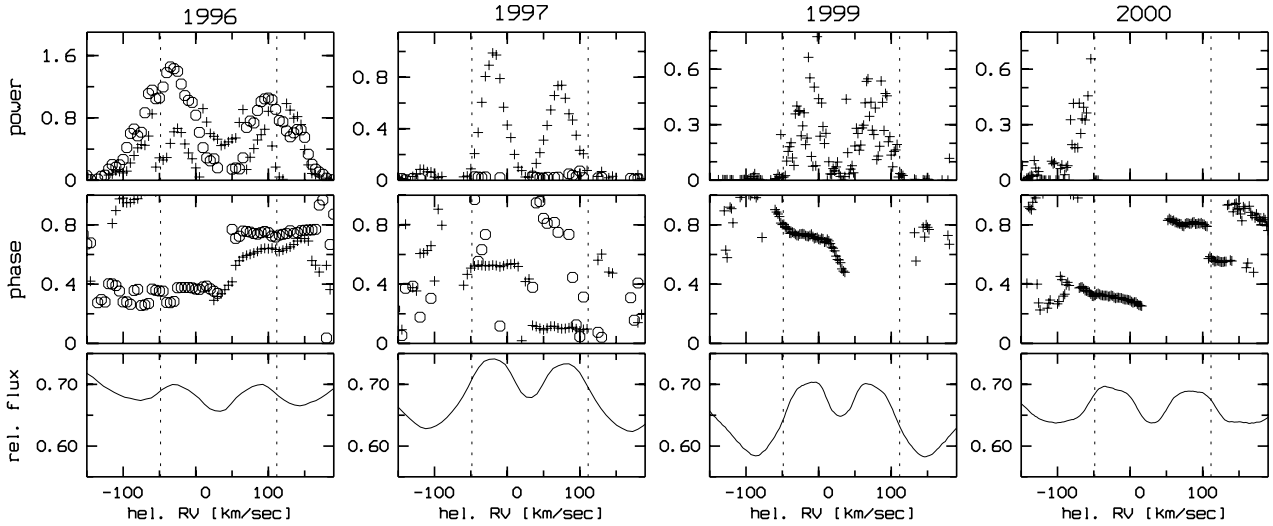

Fig. 3. Same as Fig. 2 but for Hδ. Because of insufficient frequency resolution, power and phase distribution of the 1.49-d period cannot be derived for 1999 and 2000, for which only parameters corresponding to the 1.37-d period are plotted. Significant season-to-season variations in phase distribution can be seen.

and a search for possible additional periods was done with the help of the CLEAN-type procedure described by Kaufer et al. (1997).

TSA's for different spectral lines give very consistent results. Strong power is found for the known 1.37-d period. But after subtracting this period and its harmonics in the power spectrum, no other peak remained above the 3σ level. The power of any secondary peak is lower by 3 orders of magnitude than that of the 1.37-d period. The mode variations of all measured spectral lines can be described with high accuracy as single periodic and coherent in the period 1996–2000. No indication of multiperiodicity similar to the one detected in μ Cen by Rivinius et al. (1998a) was found to the limit of the frequency resolution of 0.004 d^{-1}. This is almost one order of magnitude smaller than the typical separation of the periods in the 0.5-d group of periods in μ Cen.

By inspecting the phase diagrams and from the fitted sinusoids it was verified that there is no phase shift between the mode variations of H I, He I, Ne I, Mg II, Si II and Si III.

The final value of the period was computed as the mean of the periods derived for fifteen lines of He I and one each of Mg I, Ne I and Si III (Table 2). The He I 4922 line is blended with emission lines of Fe II. Consequently its modes show larger scatter compared with other lines and the derived period deviates from other He I lines. The modes of He I 7065 are influenced not only by blends in the stellar spectrum but also by strong telluric lines. In fact, a reliable phase diagram could be derived only for the 1996 season. The He I 4922 and 7065 lines were, therefore, excluded from the determination of the mean period.

Apart from using the modified MIDAS routines mentioned above, an independent TSA was performed by a formal application of the FOTEL code (Hadrava 2002). FOTEL, developed for the calculation of orbital parameters of binary stars, can also derive non-sinusoidal solutions. The results of the methods agree to within their errors. This confirms that the mode variations are well approximated by sinusoids as assumed in the previous step.

The ephemeris derived with FOTEL from the normalized modes of 18 spectral lines observed between 1996 and 2000 (cf. Table 2) is:

$$T_{\mathrm{RV,max}} = (2\,450\,836.780 \pm 0.007) + N \times (1.371963 \pm 0.000010). \quad (1)$$

3.3. Modes of Si II and higher Balmer lines

Higher lines of the Balmer series exhibit considerably more noise in the phase diagrams than the ones of the lines do that were used for computing ephemeris (1), particularly in the 1996 season. This can be explained by two facts: I) The amplitude of the H I modes is on average 10 times lower than the ones of the other ions in Table 2. II) The transient 1.49-d period and other, long-term variations influence the position even of the absorption cores of H I lines. Consequently, the errors of the 1.37-d period are about 10 times larger for these lines than for the other ions in Table 2. For this reason, the H I lines were not included in deriving the mean period.

In order to test the latter effect, a Fourier analysis of the modes of the H I 3734, 3750, 3770 Å lines was performed. Figure 5 shows large season-to-season variations of the corresponding power spectra. In 1996, during the state of high brightness, the 1.49-d period was also detected, with the same value as in the wings of other lines with a circumstellar contribution (Figs. 1 and 3). Its power was comparable to the one of the 1.37-d period. The mean period derived from the above mentioned three H I lines is (1.4946 ± 0.0003) d. In the same lines but the following seasons, when the visual brightness had declined, only the photospheric 1.37-d period was detected.

The Si II 6347 and 6371 lines exhibit a complicated profile structure with strongly variable absorption and emission components. Modes of the central absorption and parameters of the emission cannot be measured in all profiles. Their Fourier

Table 2. Amplitudes and γ-velocities (both in km s^{-1}) of mode variations of absorption lines; they were derived by fitting sinusoids as described in Sect. 3.1 and are listed separately for each observing season. The lines marked with an asterisk following the wavelength were used for the computation of the mean ephemeris (1) provided in Sect. 3.2. Missing values are due to either large deviations of the phase diagram from a sinusoid or a large scatter of the values derived from an ambiguously defined line core; all lines affected by this have a significant, variable emission component.

Ion	λ	1996		1997		1999		2000	
		Ampl.	γ	Ampl.	γ	Ampl.	γ	Ampl.	γ
H I	3734.370	12.9 ± 1.9	32.9 ± 1.3	3.5 ± 0.3	30.3 ± 0.2	5.5 ± 0.8	31.7 ± 0.6	8.2 ± 1.1	35.2 ± 0.8
H I	3750.154	14.3 ± 2.5	42.1 ± 1.7	3.9 ± 0.3	33.6 ± 0.2	4.1 ± 0.4	32.0 ± 0.4	9.9 ± 1.7	29.4 ± 1.2
H I	3770.632	14.9 ± 2.0	37.2 ± 1.4	4.4 ± 0.2	36.7 ± 0.2	4.5 ± 0.4	32.7 ± 0.3	6.4 ± 1.0	35.1 ± 0.7
He I	3819.606 ⋆	22.0 ± 0.6	27.3 ± 0.4	14.6 ± 0.3	27.5 ± 0.2	16.9 ± 0.4	28.0 ± 0.2	18.3 ± 0.4	28.9 ± 0.3
He I	3926.530 ⋆	23.7 ± 1.0	40.9 ± 0.7	14.6 ± 0.5	41.0 ± 0.3	16.5 ± 0.5	42.3 ± 0.4	18.9 ± 0.5	41.2 ± 0.4
He I	4009.270 ⋆	22.0 ± 0.7	36.0 ± 0.5	14.3 ± 0.3	36.5 ± 0.2	16.9 ± 0.3	36.3 ± 0.2	17.8 ± 0.3	36.2 ± 0.2
He I	4026.200 ⋆	23.6 ± 0.7	25.6 ± 0.5	14.2 ± 0.2	24.1 ± 0.1	20.4 ± 0.6	24.3 ± 0.4	20.7 ± 0.6	24.8 ± 0.4
He I	4120.800 ⋆	26.5 ± 0.7	30.6 ± 0.5	22.2 ± 0.4	33.2 ± 0.3	35.5 ± 1.1	33.0 ± 0.8	34.1 ± 0.9	33.4 ± 0.6
He I	4143.759 ⋆	20.8 ± 0.7	34.6 ± 0.4	13.8 ± 0.2	34.3 ± 0.2	18.5 ± 0.4	34.5 ± 0.3	20.8 ± 0.4	33.8 ± 0.3
He I	4168.971 ⋆	24.2 ± 1.5	34.0 ± 1.0	18.6 ± 0.5	30.8 ± 0.4	25.6 ± 1.9	29.1 ± 1.4	30.1 ± 1.1	29.8 ± 0.8
He I	4387.928 ⋆	24.5 ± 0.7	30.0 ± 0.5	15.9 ± 0.2	29.0 ± 0.1	19.5 ± 0.4	28.3 ± 0.3	23.4 ± 0.7	28.1 ± 0.5
He I	4437.550 ⋆	27.3 ± 1.2	30.3 ± 0.8	22.2 ± 0.5	31.0 ± 0.4	36.2 ± 2.0	30.3 ± 1.4	36.4 ± 1.1	29.9 ± 0.7
He I	4471.477 ⋆	31.2 ± 0.8	27.6 ± 0.6	20.7 ± 0.3	27.4 ± 0.2	35.0 ± 1.2	30.6 ± 0.8	31.9 ± 0.9	31.2 ± 0.7
He I	4713.200 ⋆	32.2 ± 1.0	31.4 ± 0.7	26.1 ± 0.4	31.0 ± 0.3	38.2 ± 1.2	30.2 ± 0.8	34.7 ± 0.8	29.5 ± 0.6
He I	4921.929	17.0 ± 0.9	12.7 ± 0.6	15.0 ± 0.4	21.8 ± 0.3	31.5 ± 1.1	27.6 ± 0.8	34.3 ± 1.1	29.4 ± 0.8
He I	5015.680 ⋆	31.1 ± 1.2	22.5 ± 0.8	29.2 ± 0.5	26.7 ± 0.4	44.0 ± 1.3	27.3 ± 0.9	39.3 ± 1.0	27.8 ± 0.7
He I	5047.739 ⋆	33.0 ± 1.4	27.8 ± 1.0	25.5 ± 0.6	26.9 ± 0.4	34.5 ± 1.1	24.2 ± 0.7	33.4 ± 0.9	25.7 ± 0.6
He I	5875.700 ⋆	35.5 ± 0.9	28.7 ± 0.6	25.5 ± 0.5	28.8 ± 0.4	38.2 ± 1.3	30.5 ± 0.9	31.1 ± 1.0	30.2 ± 0.7
He I	6678.150 ⋆	41.3 ± 1.0	30.0 ± 0.7	30.2 ± 0.6	30.4 ± 0.4	44.5 ± 1.3	29.7 ± 0.9	40.1 ± 1.0	30.4 ± 0.7
He I	7065.190	33.5 ± 1.6	30.1 ± 1.1						
Ne I	6402.246 ⋆	51.6 ± 1.6	27.4 ± 1.1	44.8 ± 1.1	28.4 ± 0.8	53.5 ± 1.4	29.6 ± 1.0	49.6 ± 1.3	29.1 ± 0.9
Mg II	4481.137 ⋆	39.7 ± 1.3	33.5 ± 0.9	32.4 ± 0.5	33.9 ± 0.4	48.2 ± 1.3	34.6 ± 0.9	43.3 ± 1.1	34.4 ± 0.7
Si II	6347.109	44.5 ± 2.0	23.9 ± 1.4	44.5 ± 2.0	23.9 ± 1.4	52.9 ± 2.2	26.3 ± 1.6	47.0 ± 1.5	27.0 ± 1.1
Si II	6371.372	50.0 ± 2.5	31.9 ± 1.7	34.5 ± 1.8	29.0 ± 1.3	54.9 ± 2.2	28.0 ± 1.6	48.1 ± 1.6	29.4 ± 1.1
Si III	4552.616 ⋆	31.6 ± 1.3	25.1 ± 0.9	25.1 ± 0.7	28.7 ± 0.5	41.1 ± 1.6	25.4 ± 1.2	42.6 ± 1.2	26.5 ± 0.8

analyses have larger errors than those of the H I modes described above. However, the power peaks of the transient period are unambiguously defined at a level of about 5% of the power of the 1.37-d period. The mean transient period of the two Si II lines is lower by about 2% than the one of the three H I lines. It is not possible to decide if the difference is real or the H I and the Si II lines are differently influenced by a conceivable convolution of the variations of the absorption and the emission components.

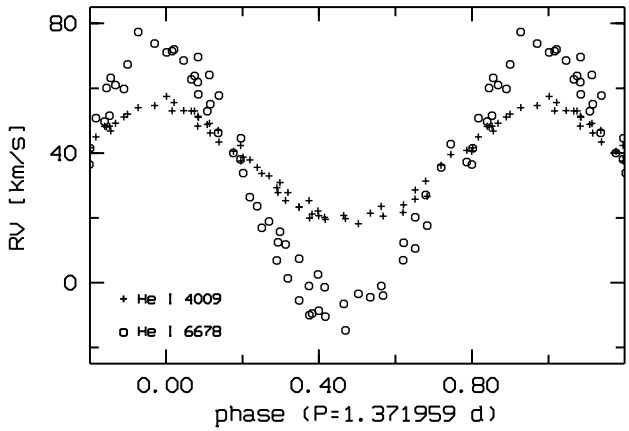

Fig. 4. RV curves (folded with the 1.37-d period) of He I 4009 and 6678 Å measured in the FEROS spectra from 2000. Note the difference in RV amplitude even between lines of the same ion.

4. Time series analysis of emission lines

In order to characterize the effect of the transient 1.49-d periodicity on standardly used emission line parameters and to localize the place of origin of this period in the extended stellar atmosphere, also a number of emission lines were subjected to a TSA. To this end, radial velocities and emission strengths were measured in double-peaked profiles of Fe II 4233, 4508, 4549, 5169, and 5316, O I 8446, Hα, Hβ, Hγ, Hδ and H I 8545. For the first three Fe II lines, the emission was of sufficient strength only in 1996 and 1997. Analysis of the single-peak Hα emission was limited to the same time interval, because a double peak structure developed in the line after 1997.

Table 2. Continued for the year 2002.

Ion	λ	2002	
		Ampl.	γ
H I	3734.370		
H I	3750.154		
H I	3770.632		
He I	3819.606 ⋆	34.7 ± 0.4	27.9 ± 0.7
He I	3926.530 ⋆	29.7 ± 0.6	37.8 ± 0.6
He I	4009.270 ⋆	26.2 ± 0.2	34.7 ± 0.2
He I	4026.200 ⋆	26.6 ± 0.5	24.2 ± 0.4
He I	4120.800 ⋆	43.0 ± 0.8	27.3 ± 0.6
He I	4143.759 ⋆	23.9 ± 0.3	29.0 ± 0.2
He I	4168.971 ⋆	28.2 ± 0.5	29.0 ± 0.4
He I	4387.928 ⋆	29.2 ± 0.3	26.9 ± 0.2
He I	4437.550 ⋆	36.1 ± 0.6	28.0 ± 0.5
He I	4471.477 ⋆	46.2 ± 0.5	28.9 ± 0.4
He I	4713.200 ⋆	41.1 ± 0.4	27.6 ± 0.3
He I	4921.929	13.2 ± 1.2	12.9 ± 0.9
He I	5015.680 ⋆	41.4 ± 0.8	22.7 ± 0.6
He I	5047.739 ⋆	36.1 ± 0.5	23.5 ± 0.4
He I	5875.700 ⋆	44.0 ± 1.0	26.6 ± 0.8
He I	6678.150 ⋆	51.2 ± 0.6	26.5 ± 0.5
Ne I	6402.246 ⋆	54.2 ± 0.8	31.1 ± 0.6
Mg II	4481.137 ⋆	48.1 ± 0.3	35.6 ± 0.2
Si II	6347.109		
Si II	6371.372		
Si III	4552.616 ⋆	42.4 ± 0.9	19.7 ± 0.7

Table 3. Amplitudes and γ-velocities (both in km s^{-1}) of mode variations of He I 4471 and Mg II 4481 lines observeded by Baade (1984) – data set A in Paper I – and He I 6678 line published by Štefl et al. (2000a) – data sets B and C – were used.

Data set	Ion	λ	Season	Amplitude	γ
A	He I	4471	1982/3	35.4 ± 2.2	29.4 ± 1.5
A	Mg I	4481	1982/3	45.5 ± 2.1	35.7 ± 1.4
B	He I	6678	1994	51.2 ± 1.8	26.9 ± 1.2
C	He I	6678	1996	49.3 ± 0.2	29.6 ± 0.2

4.1. V/R variations

In 1996, when the visual brightness was maximal, the bi-periodic character can be recognized also in the V/R variations measured in the following 7 lines: Fe II 4233, 4508, 4549, 5169, and 5317, O I 8446 and H I 8545. Figure 5 shows the power distribution for Fe II 5316 as an example. The mean value of the transient period in 1996, derived from all seven lines, is (1.482 ± 0.012) d.

In no line the transient period could be detected after 1996. By contrast, the 1.37-d period is present in all lines except for H I 8545 in 1996, 4 lines in 1997, and Fe II 5169 and O I 8446 in 1999 and 2000. However, because of the lower number of spectra and their temporal distribution, the TSA frequency resolution is considerably lower in 1999 and especially 2000.

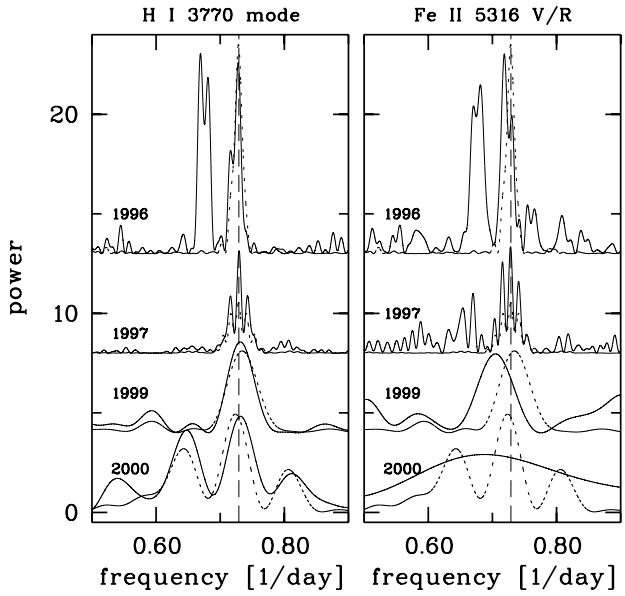

Fig. 5. Fourier power spectra of H I modes and Fe II V/R variations in various observing seasons as labeled. The power distribution of the photospheric Ne I 6402 line is overplotted as a dotted line. The dashed lines mark the frequency corresponding to the 1.37-d period. Both panels show the same long-term variations of the periodicity. The transient 1.49-d period is of the same strength as the 1.37-d period in the 1996 season, but completely disappears from the periodogram in the following seasons. Note that the side lobes in 1999 and 2000 are due to aliasing as a result of insufficient temporal coverage; they are not transient periodicities.

The variability measured in the emission lines combines variations of the underlying, although filled-in, absorption and of the emission component. Generally, the absorption component carries the 1.37 d period whereas the transient 1.49-d period influences more the emission part. This simplified picture is supported, e.g., by H I 8545, which has a strong circumstellar emission component but only very weak stellar absorption; it only showed the transient period, which moreover was restricted to 1996.

4.2. Mode variations of single-peak emission lines

The Hα emission consists of a single peak in 1996 and 1997, thereafter a double-peak structure developed. Modes of the single emission peak possess TSA properties very similar to those of the V/R variations described in Sect. 4.1 and of the modes of higher Balmer lines (Sect. 3.3). The 1996 transient period is 1.492 d.

5. Sharp absorption spikes

The most conspicuous component of the periodic *lpv* of ω CMa, the so-called spikes, was described already by Baade (1982) for the Mg II 4481 line. Meanwhile, similar features were found in HR 4074 (Baade 1984), μ Cen (Rivinius et al. 1998a) and other low $v \sin i$ Be stars (Rivinius et al. 2002).

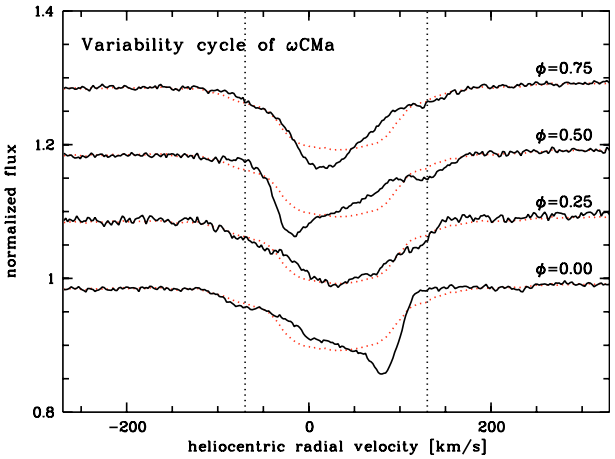

Fig. 6. Phases of symmetry and most pronounced asymmetry in the 1.37-d variability cycle of ω CMa, shown for Mg II 4481 in the 1999 data. Phase runs upward. The dotted vertical lines mark the range $\pm v \sin i$, while the dotted spectrum is the mean of all 1999 profiles.

Spikes are very narrow absorption components that develop during the phases of the 1.37-d period when the line profiles are the most asymmetric, i.e. in each cycle on the blue as well on the red side of the profiles (Fig. 6). Simultaneous to the occurrence of a spike on one side, an extended absorption "ramp" appears on the other side of the profile. The additional absorption in the ramp is shallow, but reaches beyond $v \sin i$ by several $10\,\mathrm{km\,s^{-1}}$, which is a substantial fraction of $v \sin i$. In a given spectral line, there is only one spike/ramp pair at any one time. The phases are the same for all lines.

Although the basic appearance of the *lpv* is the same in all lines, the 1999 FEROS spectra permit pronounced differences to be seen (Fig. 7). First, the spikes become narrower with increasing ion weight. In fact, spikes are not much broader than the thermal width of the respective ions. Second, the spikes are strongest (relative to the rest of the line) in lines that become stronger toward temperatures lower than the mean $T_{\rm eff}$ (e.g. S II). Lines at maximum strength around the spectral type of ω CMa have less pronounced spikes. Finally, Si III, which attains its maximum strength only at still higher temperatures, hardly shows any spike at all.

6. Discussion

The period derived in Sect. 3.2 agrees remarkably well with the "mean period" of 1.371906 d derived by Harmanec (1998). Although the difference is almost three times as large as predicted by the formal errors, both values are very close to one another. While Harmanec derived the period from the times of RV maxima/minima over a few decades, the period in this paper is based on all normalized RVs obtained between 1996 and 2000. The consistent value of the period, obtained with somewhat different methods and from different time intervals, thus makes it one of the most accurate and stable ones available for the short-time variability of any Be star. However, a more detailed analysis indicates that the true behavior is more complex than a single number can express. In particular, the meaning of the term "period" needs to be qualified.

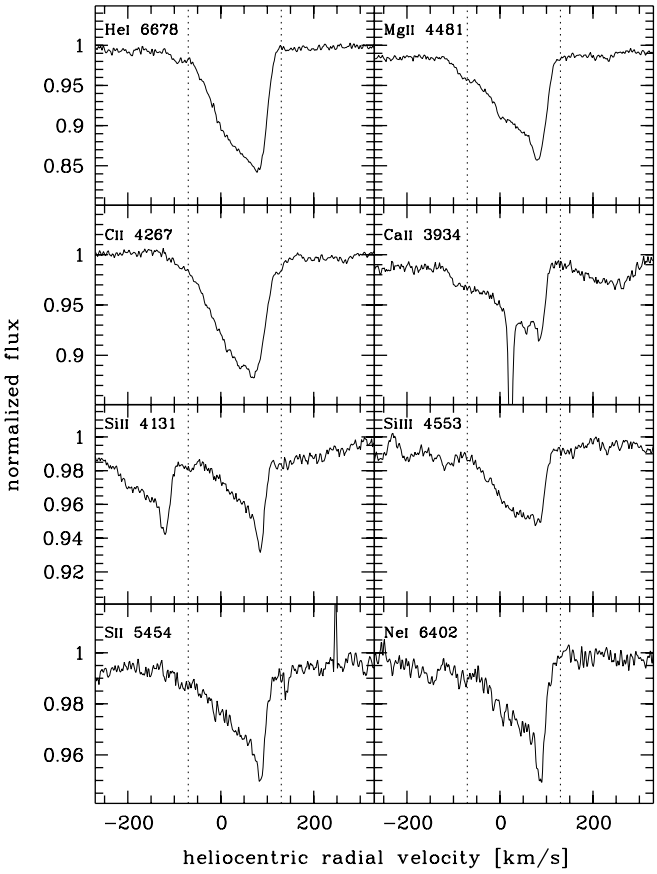

Fig. 7. Appearance of spikes in different lines. Features like those seen in the line centers of Mg II 4481 and Ca II 3934 are due to blends or interstellar absorption, however.

6.1. The nature and long-term coherency of the 1.37-d period

Harmanec (1998) found deviations of some RV maxima from a linear ephemeris. He concluded that the period itself varies cyclically or periodically with an amplitude of (0.174 ± 0.017) day on a time scale of either 5650 or 34 days, which he could not distinguish between. The following first considers the longer of the two time scales: The observations in 1996–2000 as reported in this paper span about 25% of the hypothetical 5650-d cycle. According to Harmanec's analysis, the period should have been varying between about 1.3362 and 1.4076 d. A simple estimate shows that such a period change would lead to a phase shift growing to a few cycles w.r.t. ephemeris (1) during 1996–2000. This is evidently inconsistent with the observations.

If the period varies on a 34-d time scale, the present observations would cover the range in period variation completely and the corresponding phase shifts would be even larger. Because parameters of Harmanec's cyclic variations are presented only as a formal best fit, accurate values of the expected phase shifts need not to be computed here. But it is obvious that the phase shift predicted by Harmanec's hypothesis of the variable period is inconsistent with the phase scatter of only 0.05–0.10 cycles over the interval 1996–2000 as shown in Fig. 8. Within the errors of ephemeris (1), the

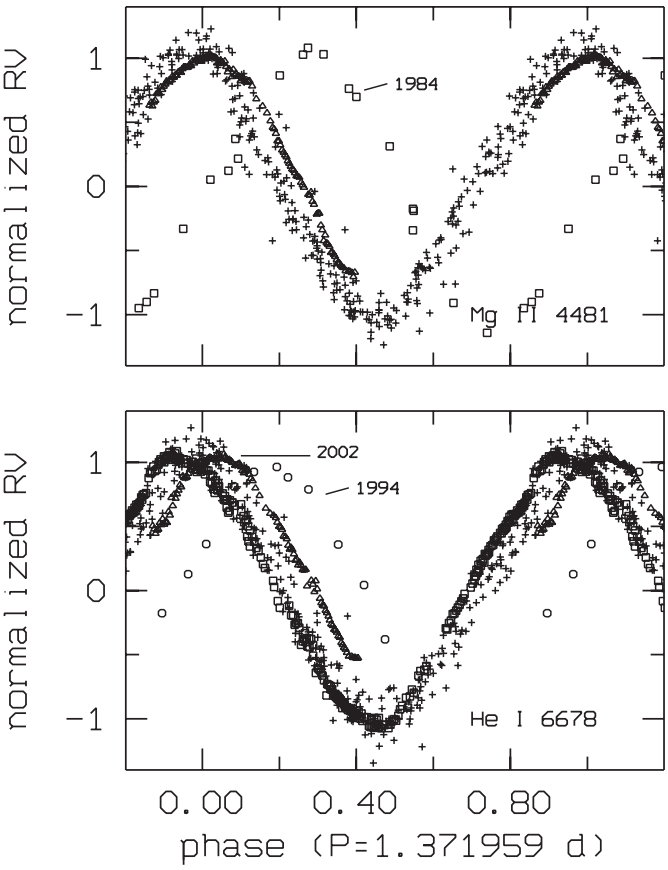

Fig. 8. The low scatter in phase diagrams of He I 6678 and Mg II 4481 modes documents a high coherency between 1996 and 2000 (+ symbols). However, a phase shift of the modes in 2002 (△ symbols) is higher by one order of magnitude than can be expected from the analysis of the 1996−2000 data. Even more conspicuous phase shifts, inconsistent with the coherency in the 1996−2000 time interval, can be seen for the 1994 modes of the He I 6678 profiles published by Štefl et al. (2000a) (○ symbols in the lower panel) and the Mg II 4481 data obtained in 1982 by Baade (1984) (□ symbols in the upper panel). Baade's He I 4471 profiles show the same phase shift as does Mg II 4481.

period is constant in the interval 1996–2000 and cyclic variations, at least with the amplitude and time scales predicted by Harmanec, can be excluded. Note that the small difference between Harmanec's "mean period" and ephemeris (1) is irrelevant for this conclusion.

On the other hand, Fig. 8 proves that the phase progression was indeed not linear outside the 1996–2000 interval. This is manifest from the following:

- Most of the scatter in the 1996–2000 interval ("+" symbols) is due to the 1996 season.
- All RVs from 2002 are shifted by about +0.1 cycles w.r.t. the mean RV curve in 1996–2000. This is larger by about one order of magnitude than what can be expected from the cycle-to-cycle variations and normalization errors.
- The RVs of the He I 6678 line in 1994 (Štefl et al. 2000a) are shifted by +0.2 (or −0.8) cycles w.r.t. the 1996 data by the same authors as well as to the mean 1996–2000 phase curve.
- The RVs of He I 4471 and Mg II 4481 in 1982 (Baade 1984) are shifted by about +0.35 (or −0.65) cycles (and possibly by an additional number of full cycles) w.r.t. the mean 1996–2000 RV curve.

6.2. Changes of phase and/or period during outbursts

Figure 8 and the above list suggest that a non-linearity in RV phase takes place during periods of high brightness, more probably at their beginning. However, the amount of data is not sufficient to clarify whether the phase jumped at constant period or whether the period was slightly different temporarily, thereby causing a phase drift.

As will be shown in Paper III of this series, the 1.37-d *lpv* underlying the RV variations is due to non-radial *g*-mode pulsation. Therefore, the RV phase is nothing but a position angle of the *nrp* surface velocity pattern which propagates w.r.t. the observer. There is hardly any physical justification to make this angle jump discontinuously. However, the period of a non-radial pulsation mode can change due to at least two effects.

First, the frequency of *g*-modes is inversely proportional to the stellar radius. The early phase of a Be star outburst, independent of the physical process leading to it, can most probably be crudely imagined as some expansion of the photosphere, conceivably limited to low stellar latitudes. As a result, the surface velocity pattern requires more time between two passages of the observer's substellar point. As a second result, and possibly helped by some further unknown process, matter is ejected to the circumstellar disk. Thereafter, the previous values of the stellar radius and, consequently, of the pulsational period as well are restored. However, during the time interval when the period was longer, some phase difference was accumulated relative to the case if the pulsation had not been disturbed by the outburst.

Second, the pulsation frequency is also sensitive to changes in the boundary conditions. For a stable wave to develop, the disturbance caused by the driving mechanism has to be reflected at the outer boundary, which is the stellar surface. During periods of low brightness, which are far away from those of outbursts, circumstellar disk and star are spatially separated (Rivinius et al. 2001a). Then, any structural changes in the disk will not have an appreciable effect on the star. This is consistent with the period and phase having remained stable and coherent from 1996 to 2000 (when ω CMa was close to its photometric ground state). At times of high brightness, however, the disk is replenished with matter ejected by the star and the two can interact with one another directly. This will change the outer boundary condition for the pulsational driving. The resulting so-called "wave leakage" has been explored as a potential *nrp*-driven mass-loss mechanism. But primarily only effects observable in the line profile variability were investigated, not changes of the stellar eigenfrequencies (Townsend 2000).

The phase difference between 1996–2000 and 2002, when the pulsation was a bit "late", suggests a slightly longer period at times of high brightness. The implied temporary change in period is only of the order of a few thousandths or hundredths.

When the disk becomes detached from the star again, i.e. when the outburst has ended, the outer boundary conditions return to their old state. Accordingly, also the period recovers its value of the previous time of low brightness and stellar quiescence. Therefore, the mean period of Harmanec (1998) and the period of ephemeris (1) are in agreement.

The two results also have in common that there is some apparent variation of the period. The present study is limited to less than one cycle in visual long-term brightness variation. The suspected relation between the variations in brightness and pulsational period therefore prevents a test whether the variation of the period is cyclic. By contrast, Harmanec analyzed RVs obtained over several decades, during which several outbursts and brightening cycles should have occurred, so that he could perform such a test. From the present data, Harmanec's short cycle length of 34 days is excluded. The longer one, 5650 days or 15.5 years, is about twice the photometric long-term cycle of 7–9 years derived in Paper I. The results of the present study make it unlikely that the variation in RV phase is due to the varying light travel time in a binary orbit. Rather, it appears to be due to the interaction between two intrinsic variabilities of a single star.

6.3. Photospheric vs. circumstellar origin of the 1.37-d periodicity

In the absence of interferometrically aided spectroscopy, the place of origin of the *lpv* can only be inferred indirectly in an extended atmosphere. Recently, it was claimed (Balona et al. 2001) that variability of spectral lines filled in by emission would identify the location of the *lpv* as exo-photospheric. But no evidence was added in support of this belief.

In the case of ω CMa, the 1.37-d *lpv* of Si III 4553 was the same in 1996, 1997, 1999, 2000, and 2002, i.e. over the full range of visual brightness and mass loss activity. Therefore, either the *lpv* mechanism is fully inert against this long-term variability or it originates mainly from where there was less of this variability. This is clearly the photosphere. The photospheric origin is also strongly preferred by the nature of this Si III transition, which has a lower level with an excitation energy of about 19 eV. A B2 star would be very ineffective in significantly populating this level in the disk when the latter is well detached from the star. In fact, even in strong early-type shell stars like ζ Tau, this line does not appear in shell absorption or emission.

Figure 9 demonstrates beyond any reasonable doubt that the 1.37-d *lpv* of O I 8446, Fe II 5169 and Hδ is the same as the one of Si III 4553: only during outbursts were there differences (for a discussion of this difference see Sect. 6.4). Not only does this show that the *lpv* of all these lines has the same, namely photospheric, origin but any additional exo-photospheric contribution must be small: The 3 lines other than Si III 4553 do have a large exo-photospheric part (cf. Sect. 2.1) and so should be much more sensitive to any exo-photospheric component of the *lpv*; this is not observed.

Finally, independent evidence in support of the photospheric explanation comes from the B2 IV-Ve star HR 4074. Not only does it have about the same spectral type as ω CMa but also nearly the same $v \sin i$ and *lpv*. But line emission was last observed more than 100 years ago. Accordingly, there is no appreciable quantity of exo-photospheric matter that could contribute to the *lpv* (Štefl et al. 2002). This implies that the plentiful circumstellar matter around ω CMa is unimportant for the 1.37-d *lpv*.

6.4. Outbursts and the 1.37-d line profile variability

During the monitoring period of 1996 to 2002, the outbursts observed in early 1996 and early 2002 were the only occasion when the circumstellar disk was in contact with the photosphere. In all other seasons, the properties of optically thin emission lines, mainly their decreasing base width after outbursts, suggest a local density minimum of variable width between the stellar surface and the inner edge of the circumstellar disk (Rivinius et al. 2001a). The most quiescent season in terms of emission variability and the one when the density gap was largest was in 1999.

At the times of the closest contact between star and disk, the *lpv* of some lines deviates considerably from the template *lpv* of Si III4553 (cf. Fig. 9). The main temporary feature is the strong dominance of red-to-blue, i.e. retrograde travelling features, which were already reported by Baade (1982). It seems that this mainly concerns lines with a strong circumstellar component (marked "sc" in Table 1). During an outburst, photosphere and disk are in contact with one another, meaning that the disk could occult the circumequatorial part of the photosphere. For transitions with considerable optical depth this could result in the underlying photospheric component being largely veiled. Preliminary, purely parametric tests, in which some equatorial strip is artificially discarded when integrating the observed profiles across the visible stellar disk, leave open the possibility for an explanation of this kind.

Rivinius et al. (1998b) showed that the emission line outbursts of the Be star μ Cen are triggered by the beating of at least two of the strongest *nrp* modes. ω CMa seems to be strictly single-periodic at the photospheric level. Yet, it regularly undergoes major outbursts (or series of minor outburts). Therefore, the beating of *nrp* modes is only one of several mechanisms that can trigger a Be star outburst. (Since late-type Be stars do not seem to undergo outbursts, their share of the Be phenomenon would anyway require a different explanation.)

6.5. Transient periodicities

It seems that in ω CMa transient periodicity is detectable during visually bright phases only. This conclusion finds a firm support in the 1996 data, when the star was bright. It is consistent with the non-detection in 1997, 1999, and 2000. But in 2001/2, when the star was again bright, the data sampling was insufficient. Only the perturbation of the 1.37-d *lpv* was similar as in 1996. Moreover, in μ Cen (Rivinius et al. 1998a), transient periods were regularly detected during outbursts.

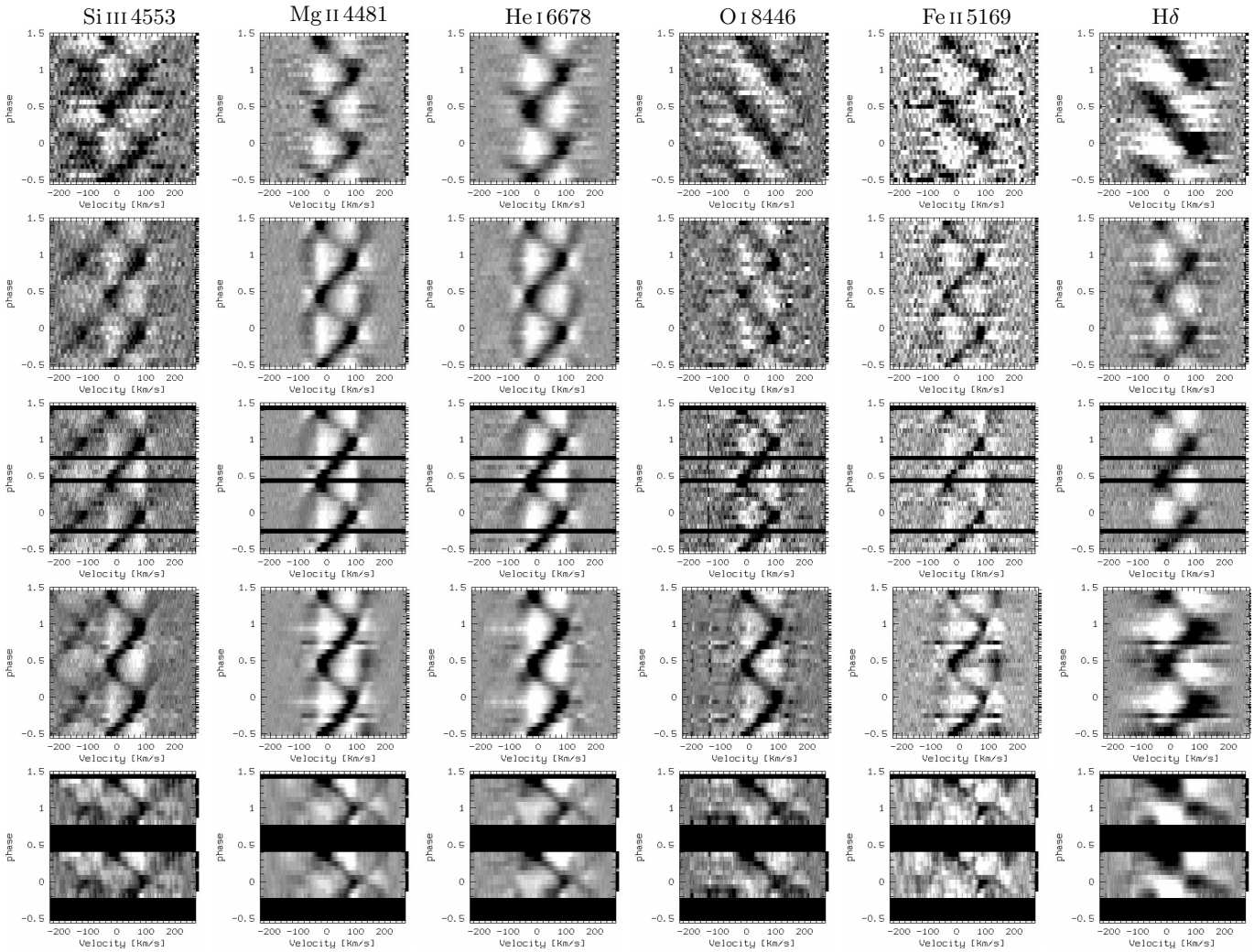

Fig. 9. *lpv* residuals of selected spectral lines (as labeled) in 1996, 1997, 1999, 2000, and 2002 (rows from top to bottom). The 1996 and 1997 observations were obtained with HEROS, those since 1999 with FEROS. The line with the least circumstellar contribution, Si III 4553, shows identical *lpv* in all seasons (both wings are blended with Fe II lines). When the disk is in quiescence (and probably well detached from the stellar surface as in 1997, and even more so in 1999) also the other spectral lines show the same *lpv* pattern. Only in, or close to, outburst phases (1996) seem lines with significant emission contribution to exhibit a different *lpv*. The conversion from intensity to greyscale is kept constant for each spectral line to enable variations in the *lpv* amplitude to be seen.

This study of ω CMa also confirms the conclusions by Štefl et al. (2002) that the presence of transient periods can seriously perturb and, in fact, falsify time series analyses if they are not properly accounted for.

The nature of the transient periods is not known. By contrast to the 1.39-d period, the transient 1.49-d period is found in lines with dominant circumstellar origin but not in as nearly purely photospheric lines as Si III 4553. This means that the reverse of the arguments in Sect. 6.3 applies and this transient period probably resides more nearly in the disk than in the photosphere (Štefl et al. 2002).

One may wonder whether they represent some echos of the photospheric *nrp* in the inner part of the disk at times when photosphere and disk are in closer contact and so can interact more strongly. However, so far no quantitative model has been elaborated assessing the damping effect of the dynamic instabilities in the disk and other physical conditions important for the driving of transient pulsations in the disk. Current observations do not provide all parameters needed for such a study, e.g. the inner radius and density profile of the disk during as well as their variations with phase of the outburst cycle.

6.6. Absorption spikes

The width of these features does not significantly exceed the thermal broadening (Sect. 5). Therefore, rotation cannot be essential for their occurrence, given their rather large equivalent width requiring a proportionally large fraction of the stellar surface for their formation. This can only be accomplished by means of some additional velocity field.

Owing to the rapid rotation, the so-called gravity darkening causes the equator of a Be star to be cooler than its pole.

Accordingly, the sequence of relative spike strength derived in Sect. 5 represents also a spatial sequence of line formation from equator (strong spike) to pole (weak spike), assuming that spikes are formed in the photosphere.

These properties were already successfully modelled for μ Cen (Rivinius et al. 2001b) and preliminarily for ω CMa as well (Maintz et al. 2000). They are just the consequence of nonradial pulsation in a rapid rotator viewed pole-on. This will be explained in detail, incl. line-to-line differences, in Paper III of this series.

7. Conclusions

The primary challenge in understanding ω CMa lies in properly isolating the mean short-period variability in the presence of strong, a-periodic long-term modulations. A second one arises from the pronounced line-to-line differences. However, it is also evident that these, at a first glance, annoying complications also offer the potential of additional diagnostics.

An attempt to provide a simplified road map (formerly: hitch hiker's guide) to the labyrinth of ω CMa's variability is undertaken in the following:

- o There are a permanently present period of 1.37-d and a transient period near 1.49-d. Both can be derived from RV (mode) measurements. Many lines are affected by both periods, albeit at different relative strengths. Few other lines only show the one or the other.
- o In the absence of major outbursts, the 1.37-d period is phase coherent over several years. The length of such quiescent phases is insufficient to resolve this period into two or more closely spaced ones.
- o At times, drifts of the phase of the 1.37-d variation occur. They seem to be associated with major outbursts when the star is visually bright and presumably in contact with the circumstellar disk. This can be described as a temporary increase of the period by a few thousandths or hundredths. After the outburst, the orginal period is restored. Assuming an *nrp* model, one may attribute this to a temporary increase in radius of the star or the outer boundary layer of the pulsation.
- o The most conspicuous detail of the 1.37-d variability is the development of a narrow spike near one wing and of a ramp considerably extending the other wing beyond the stellar $v \sin i$. Half a cycle later, the profiles are mirrored about their center.
- o Amplitudes and γ-velocities of 1.37-d period differ strongly among the spectral lines even for one and the same ion. On time scales of some months they are variable.
- o The most uniform and persistent variations are due to the 1.37-d period in lines formed in the photosphere only (Si III, Ne I).
- o Lines with both a photospheric and an exo-photospheric component still show the same *lpv* pattern regardless of the mix of these two components.
- o The two previous points identify the stellar photosphere as the origin of the 1.37-d period.
- o The transient 1.49-d period occurred during the main outburst phase in 1996. A reasoning similar to the one used for the 1.37-d period, but based on very contrary observational results, suggests that this periodicity resides mainly in the circumstellar disk. These facts are in agreement with similar observations which are only available for a few other Be stars. Transient periods may arise from star-disk interactions when the two are in contact during an outburst. But this hypothesis requires substantial further checking. Long-term TSAs of active Be stars must pay attention to the possible presence of transient periods, which can otherwise lead to severely flawed conclusions.
- o Unlike in μ Cen, there is no evidence that outbursts of ω CMa are triggered by the beating two or more nonradial pulsation modes (but Paper III will show that the 1.37-d period is due to an $\ell = 2$, $m = +2$ g-mode).

This map probably identifies and places the main features approximately correctly, and it bears similarities with maps of some other Be stars. But considerable improvements should result from series of observations extending over several activity cycles and sampling the crucial phases at higher temporal resolution.

Acknowledgements. We thank the European Southern Observatory for generous allocations of observing time and the staff at La Silla for their kind assistance during the observations. We appreciate also the sharing by the FEROS Consortium of their guaranteed observing time and the financial support of the 1999 HEROS observing run by LSW-Förderkreis. Further thanks are due to Dr. R. Townsend for helpful comments and a constructive discussion. This work was supported by the Deutsche Forschungsgemeinschaft (Wo 296/20-1, 436 TSE 113/18) and the Academy of Sciences and Grant Agency of the Academy of Sciences of the Czech Republic (436 TSE 113/18, AA3003001).

References

Baade, D. 1982, A&A, 105, 65
Baade, D. 1984, A&A, 134, 105
Balona, L. A., Aerts, C., Bozic, H., et al. 2001, MNRAS, 327, 1288
Briot, D. 1981, A&A, 103, 1
Hadrava, P. 2002, http://www.asu.cas.cz/~had/fotel.html
Harmanec, P. 1998, A&A, 234, 558
Kaufer, A., Stahl, O., Wolf, B., et al. 1997, A&A, 320, 273
Maintz, M., Rivinius, Th., Tubbesing, S., et al. 2000, in The Be Phenomenon in Early Type Stars, ed. M. A. Smith, H. F. Henrichs, & J. Fabregat, ASP Conf. Ser., 214, IAU Colloq., 175, 244
Maintz, M., Rivinius, Th., Štefl, S., et al. 2003, A&A, 411, 181 (Paper III)
Najarro, F. 1995, Ph.D. Thesis, Ludwig-Maximilian University, Munich, Germany
Rivinius, Th., Baade, D., Štefl, S., et al. 1998a, A&A, 336, 177
Rivinius, Th., Baade, D., Štefl, S., et al. 1998b, in A Half Century of Stellar Pulsation Interpretations, ed. P. A. Bradley, & J. A. Guzik, ASP Conf. Ser., 135, 343
Rivinius, Th., Baade, D., Štefl, S., & Maintz, M. 2001a, A&A, 379, 257
Rivinius, Th., Baade, D., Štefl, S., et al. 2001b, A&A, 369, 1058
Rivinius, Th., Baade, D., Štefl, S., & Maintz, M. 2002, in ASP Conf. Ser. 259, Radial and Nonradial Puslation as Probes of Stellar Physics, ed. C. Aerts, T. R. Bedding, & J. Christensen-Dalsgaard, IAU Colloq., 135, 240

Scargle, J. D. 1982, ApJ, 263, 835
Schwarzenberg-Czerny, A. 1993, in Analysis of Astronomical Time Series, ed. P. J. Grosböl, & R. C. E. de Ruijsscher, 5th ESO/ST-ECF Data Analysis Workshop, ESO Conf. and Worksh. Proc., 47, 149
Stee, P. 2000, in The Be Phenomenon in Early Type Stars, ed. M. A. Smith, H. F. Henrichs, & J. Fabregat, ASP Conf. Ser. 214, IAU Colloq., 175, 129
Štefl, S., Baade, D., Rivinius, Th., et al. 1998, in A Half Century of Stellar Pulsation Interpretations, ed. P. A. Bradley, & J. A. Guzik, ASP Conf. Ser., 135, 348
Štefl, S., Aerts, C., & Balona, L. A. 1999, MNRAS, 305, 505
Štefl, S., Balona, L. A., & Aerts, C. 2000a, J. Astron. Data, 6 (on CD-ROM)
Štefl, S., Budovičová, A., Baade, D., et al. 2000b, in The Be Phenomenon in Early Type Stars, ed. M. A. Smith, H. F. Henrichs, & J. Fabregat, ASP Conf. Ser. 214, IAU Colloq., 175, 240
Štefl, S., Rivinius, Th., & Baade, D. 2002, in Radial and Nonradial Puslation as Probes of Stellar Physics, ed. C. Aerts, T. R. Bedding, & J. Christensen-Dalsgaard, ASP Conf. Ser., 259, 248
Štefl, S., Baade, D., Rivinius, Th., et al. 2003, A&A, 402, 253, (Paper I)
Townsend, R. H. D. 2000, MNRAS, 318, 1
Tubbesing, S., Rivinius, Th., Wolf, B., & Kaufer, A. 2000, in The Be Phenomenon in Early Type Stars, ed. M. A. Smith, H. F. Henrichs, & J. Fabregat, ASP Conf. Ser. 214, IAU Colloq., 175, 232